Lattice theory of solvation in macromolecular fluids. III. Monte Carlo simulations

Roberto Olender
Department of Chemical Physics, Weizmann Institute of Science, Rehovot 76100, Israel

Abraham Nitzan
School of Chemistry, The Sackler Faculty of Science, Tel Aviv University, Tel Aviv 69978, Israel

D. Knödler and W. Dieterich
Fakultät für Physik, Universität Konstanz, 78434 Konstanz, Germany

(Received 21 February 1995; accepted 20 June 1995)

Monte Carlo simulations are used to calculate the energy, free energy, and entropy of solvation in a lattice model of polymer host. The solute particle interacts with specific beads in the host chain at nearest neighbor sites. The results are used to check the accuracy of the quasichemical approximation (QCA) recently used [Olender and Nitzan, J. Chem. Phys. **101**, 2338 (1994)] to study ion solvation and ion pair dissociation in polymer hosts. For noninteracting chains we find that the QCA is very accurate when the solvent consists of homogeneous chains (all beads interact equally with the impurity), and give errors of up to 20% when nonhomogeneous chains (with some of the beads interacting with the impurity) are used. For interacting chains this trend is reversed and the QCA works better for nonhomogeneous chains. Deviations of the QCA prediction from the ''exact'' numerical results are traced to three-body and higher order correlations. The success of the QCA for interacting solvents of nonhomogeneous chains is associated with cancellation of opposing effects of such correlations. © *1995 American Institute of Physics.*

I. INTRODUCTION

Following the increasing interest in the equilibrium properties of polymeric ionic conductors, such as the solvation and association of ions in polymeric hosts,[1] we have studied[2] these properties using a lattice theory of solvation. In particular, we have used[2(b)] Guggenheim's quasichemical approximation (QCA) (Refs. 3 and 4) to derive expressions for the thermodynamic quantities of solvation (free energy, entropy, enthalpy, and volume) at infinite dilution of the ions, and for the equilibrium constant for ion-pairing as a function of temperature, pressure, and solvent properties. We have shown that a combination of dielectric continuum theory for long range interactions together with the application of QCA for the short range interactions can be used to rationalize a range of experimental results for ions solvated in low and high molecular weight polyethers.

In the present work we examine the validity of the QCA when applied to this problem by comparing the QCA solvation energy to that obtained from Monte Carlo (MC) simulations for the same model and for various system parameters. We focus on the temperature dependence of the solvation energy, from which free energy and entropy of solvation can be obtained.

In the model considered, the ion–polymer mixture is contained in a cubic lattice characterized by a coordination number z. A molecule of type i occupies r_i connected lattice sites and interacts with all the other molecules in the mixture by site exclusion and nearest neighbor interactions. These molecules may have several kinds of ''beads,'' each interacting differently with the other components of the mixture. The lattice contains empty sites (component of type $i=0$ whose chain length is 1) which interact with the other components by site exclusion only.

The simulations are done at constant volume, and the QCA calculation is performed accordingly. Details of the QCA procedure [similar to the constant pressure calculation of Ref. 2(b)] are summarized in Appendix A.

II. QUASICHEMICAL APPROXIMATION

In this section we briefly review the QCA formalism for a general lattice gas mixture, focusing on the expressions that will be used for comparing between theory and simulations. The system considered consists of a mixture of N_i molecules of type i $(i=0,\ldots,n)$, where i denotes a particular component of the $(n+1)$-component mixture and $i=0$ refers to the empty sites. Each molecule in the mixture is made of r_i ''beads'' connected in a chainlike manner, each occupying one site on a lattice of coordination number z. By definition $r_0=1$. The volume of the system is expressed by $V=Mv^*$, where $M=\Sigma_{i=0}^{n} r_i N_i$ is the total number of sites and v^* is the average volume of a lattice site in the mixture. v^* is a constant parameter in this study. The density of component i is defined as $\rho_i=r_i N_i/M$, and is the average probability that a site is occupied by a segment of a molecule of type i.

From the QCA, the free energy of the system is given in terms of the composition $\{N_i\}$ and of the number of nearest neighbor pairs of beads of types i and j, $\{N_{ij}\}$. The Helmholtz free energy is obtained as $A(\{N_i\},\{N_{ij}\}) = E(\{N_i\},\{N_{ij}\}) - TS(\{N_i\},\{N_{ij}\})$. Here the energy E is given by the sum of terms $-N_{ij}\epsilon_{ij}$ over all types of nearest-neighbor pairs, where the interaction energies $\{-\epsilon_{ij}\}$ are constant parameters ($\epsilon_{ij}>0$ for attractive interactions). The interactions with empty sites $\{\epsilon_{i0}\}$ are zero. The entropy S is obtained from Guggenheim's formula[3,4] for the total number of configurations of the chains in the lattice [Eq. (1) of Ref.

2(b)]. From the minimization of the free energy of the system with respect to $\{N_{ij}\}$, the well-known quasichemical equation is obtained

$$4N_{ii}N_{jj}=e^{\Delta\epsilon_{ij}/kT}N_{ij}^2, \tag{1}$$

where $\Delta\epsilon_{ij}\equiv(\epsilon_{ii}+\epsilon_{jj}-2\epsilon_{ij})$. The quantities $\{N_i\}$ and $\{N_{ij}\}$ are related by[3]

$$2N_{ii}+\sum_{j(\neq i)}N_{ij}=q_i z N_i, \tag{2}$$

where the parameter q_i is defined by

$$q_i=[r_i(z-2)+2]/z. \tag{3}$$

For an unbranched chain zq_i is the number of nonbonded nearest neighbors to a molecule of type i.[3] For empty sites $q_0=1$. The total number of nonbonded pairs is $(z/2)N_q$, where $N_q\equiv\Sigma_{i=0}^{n}q_iN_i$.

Following Barker,[5] Eqs. (1) and (2) can be generalized, within the QCA, to consider chains with beads of different kinds. For simplicity consider the case where all molecules are identical chains of size r, however each chain contains several types of beads. The generalization is done by simply redefining molecular types as referring to these distinct types of beads, and the parameter zq_i then corresponds to the number of nonbonded nearest neighbor to all beads of type i in a given chain. q_i is not given now by Eq. (3), which is valid only for a whole molecule of type i, and depends on the locations of beads of type i in the chain. However,

$$\sum_i q_i=[r(z-2)+2]/z, \tag{4}$$

where the sum is over all the different types of beads in the molecule.

The set of Eqs. (1) and (2) is sufficient for determining the values of $\{N_{ij}\}$ in terms of $\{\epsilon_{ij}\}$, T, $\{zq_i\}$ and $\{N_i\}$, $(i=0,\ldots,n)$. These equations can be simplified by scaling the amount of pairs N_{ij}, as well as the total number of nonbonded nearest neighbors to molecules (or beads) of type i, zq_iN_i, by the total number of pairs $(z/2)N_q$. In terms of the scaled variables $\{\chi_{ij}\}$ and $\{\varphi_i\}$, defined by

$$\chi_{ii}\equiv\frac{N_{ii}}{\frac{z}{2}N_q},\quad \chi_{ij}\equiv\frac{1}{2}\frac{N_{ij}}{\frac{z}{2}N_q},\quad \varphi_i\equiv\frac{q_iN_i}{N_q}, \tag{5}$$

Eqs. (1) and (2) become

$$\chi_{ii}\chi_{ij}=e^{\Delta\epsilon_{ij}/kT}\chi_{ij}^2, \tag{6}$$

$$\varphi_i=\chi_{ii}+\sum_{j(\neq i)}\chi_{ij}. \tag{7}$$

The system of nonlinear Eqs. (6) and (7) can be solved exactly for a two component mixture $(n=1)$ [cf. Eq. (22) in Ref. 2(b)]. An exact solution can be also obtained for a multicomponent system in the random mixing limit, $\Delta\epsilon_{ij}/kT=0$, for any i and j, which leads to $\chi_{ij}=\varphi_i\varphi_j$ (all i and j). In the general case these equations have to be solved numerically, and this was done using the multidimensional Newton–Raphson method.[6] This iterative method can be used efficiently by starting with the known solution at $\beta=1/kT=0$, then increasing β stepwise, using the solution $\{\chi_{ij}\}$ obtained for the previous temperature as a first trial in the calculations at the new temperature.

TABLE I. Systems of noninteracting chains studied by Monte Carlo simulations. C denotes a bead which does not interact, and X a bead which interacts attractively, with the impurity. N is the number of chains in the $10\times10\times10$ lattice, ρ is the corresponding density (fraction of occupied sites), ρ_X is the density of X sites which interact attractively (at nearest neighbor distance) with the impurity. zq_X and zq_C are the number (per chain) of nearest neighbors to X sites and to C sites, respectively.

Label	Chain	N	ρ	ρ_X	zq_X	zq_C
A1	X_4	100	0.400	0.400	18	⋯
A2	X_4	130	0.520	0.520	18	⋯
A3	X_4	162	0.648	0.648	18	⋯
A4	X_{13}	40	0.520	0.520	54	⋯
A5	X_{13}	54	0.702	0.702	54	⋯
B1	$CXCC$	100	0.400	0.100	4	14
B2	$CXCC$	130	0.520	0.130	4	14
B3	$CXCC$	162	0.648	0.162	4	14
C1	$C(XCC)_2$	74	0.518	0.148	8	22
C2	$C(XCC)_4$	40	0.520	0.160	16	38
C3	$C(XCC)_4$	54	0.702	0.216	16	38
C4	$C(XCC)_8$	21	0.525	0.168	32	70
D1	$C(XCCC)_2$	58	0.522	0.116	8	30
D2	$C(XCCC)_3$	40	0.520	0.120	12	42
D3	$C(XCCC)_3$	54	0.702	0.158	12	42
D4	$C(XCCC)_6$	21	0.525	0.126	24	78

The parameters $\{\chi_{ij}\}$ obtained in this way are used to calculate thermodynamic quantities for the solvation process.[2(b)] Here we compare them with the MC simulations of the same system. We focus on the average solvation energy which is easily obtained from the simulations. The temperature dependence of this quantity is directly related to the other thermodynamic functions of solvation.

In a system containing a single solute molecule of type I (''ion'') the solute–solvent interaction energy of this impurity is given by

$$\mathscr{E}_I=\sum_i{}'\ \epsilon_{Ii}N_{Ii}=zN_q\sum_i{}'\ \epsilon_{Ii}\chi_{Ii}, \tag{8}$$

where Σ_i' denotes summation over all $i\neq I$, and χ_{Ii} is obtained from the QCA Eqs. (6) and (7). For a solvent made of noninteracting chains,[7] $\mathscr{E}_I$ is equal to the solvation energy ΔE_I. In this case $\mathscr{E}_I$ obtained from the QCA at infinite dilution takes the form (see the Appendix),

$$\mathscr{E}_I=-zq_I\frac{\Sigma_i'\epsilon_{Ii}\chi_{0i}^0e^{\epsilon_{Ii}/kT}}{\Sigma_i'\chi_{0i}^0e^{\epsilon_{Ii}/kT}}=-zq_I\frac{\Sigma_i'\epsilon_{Ii}\varphi_i^0e^{\epsilon_{Ii}/kT}}{\Sigma_i'\varphi_i^0e^{\epsilon_{Ii}/kT}}, \tag{9}$$

where the superscript 0 indicates quantities calculated for the pure solvent, i.e., with $\varphi_I=0$, and where the second equality follows from the fact that $\chi_{ij}^0=\varphi_i^0\varphi_j^0$ in the case of noninteracting chains. In the actual QCA calculations based on Eqs. (8) and (9) the system considered was the same one used in the simulation, containing a single ''ion'' in a lattice of 1000 sites. The infinite dilution result (9) constitutes an excellent approximation for this case. [For the system parameters of Table I we have found that results based on Eq. (9) differ by no more than 0.1% from those obtained from Eq. (8).]

An approximate expression for $\mathscr{E}_I$ can be obtained by making the mean-field approximation for the solvent (MFAS) as was done in Refs. 2(b) and 8. This involves taking $\epsilon_{ij}\to 0$ and $z\to\infty$ for $i,j\neq I$ (this is exact in the present system of noninteracting solvent molecules), while keeping $z\epsilon_{ij}$ constant, together with the substitutions $\chi_{ij}\to\varphi_i\varphi_j$, $q_i\to r_i$, and $\varphi_i\to\rho_i$. Under this approximation Eq. (9) becomes

$$\mathscr{E}_I^{\mathrm{MF}}=-zq_I\frac{\Sigma_i'\epsilon_{Ii}\rho_i^0 e^{\epsilon_{Ii}/kT}}{\Sigma_i'\rho_i^0 e^{\epsilon_{Ii}/kT}}. \tag{10}$$

Exact results are obtained in the limits of zero and infinite temperature. When $T\to\infty$ Eqs. (9) and (10) become, respectively, $\mathscr{E}_I=-zq_I\Sigma_i'\epsilon_{Ii}\varphi_i^0$ and $\mathscr{E}_I^{\mathrm{MF}}=-zq_I\Sigma_i'\epsilon_{Ii}\rho_i^0$. At zero temperature all the sites nearest neighbor to the ion are occupied with the bead of type $i=X$ whose attractive interaction with the ion is largest, and the solvation energy becomes $\mathscr{E}_I=-zq_I\epsilon_{IX}$.

Free energies can be obtained from the energies using standard methods. The Helmholtz free energy A of the whole system can be obtained from the temperature dependence of the average energy using

$$\beta A(\beta)-\beta' A(\beta')=\int_{\beta'}^{\beta}E(\beta)d\beta. \tag{11}$$

Similarly, the free energy of solvation, A_I, is calculated by scaling the impurity-solvent interaction by an auxiliary parameter λ and integrating the resulting $\mathscr{E}_I(\lambda)$,

$$A_I(\lambda=1)-A_I(\lambda=0)=\int_0^1\frac{\mathscr{E}_I(\lambda)}{\lambda}\,d\lambda. \tag{12}$$

Equations (11) and (12) are equivalent in the case of noninteracting chains ($E=\mathscr{E}_I$ in this case). Note that the free energy of solvation defined by Eq. (12) does not include the energy associated with cavity formation (see the Appendix).

III. MONTE CARLO SIMULATIONS

The simulated system consists of a single impurity (''ion'') and several chains of equal size in a simple cubic lattice ($z=6$). Two types of beads are considered; beads of type ''*C*'' which do not interact with the ''ion'' and beads of type X which interacts attractively with it. We use ''homogeneous chains'' where all beads are of type X, and nonhomogeneous chains consisting of beads of both types X and C. Our typical lattice is of size $10\times10\times10$. Most of the present work is concerned with solvents of noninteracting chains, although some results for interacting chains are described later.

The configurations of the system are propagated using a metropolis algorithm with kink–jump and crankshaft moves.[9] In addition, for the trial move of the end-beads we choose, with equal probabilities, any of the four directions perpendicular to the end bond of the chain. Finally, the trial moves of the ion are made into any available nearest neighbor location. For a lattice gas model of pure macromolecular melts this algorithm was shown to provide an adequate sampling of the configuration space. It was argued that it also provides a useful shortcut to dynamical properties.[10]

The initial configuration of the system is constructed by successively adding chains to the lattice up to the desired density. Each chain is constructed by randomly choosing the position of its first bead, then growing it to the final size by successively adding beads at randomly chosen sites nearest neighbor to the last bead added, until the final size is reached. If this process fails it is restarted from a different initial position. This simple algorithm cannot efficiently generate very dense configurations, particularly for long chains. For the densities and chain lengths studied in this work (see Table I), it worked well.

Following this preparation process the system was thermalized until the end-to-end distance and the gyration radius of the chains, as well as the total energy in the system, ceased to vary in a systematic way. This typically required 1000–2000 MC steps per particle, depending on the chain length. The results represented below were obtained from averages over 40–100 different MC trajectories, each with 2000 MC steps per bead (4000 steps per particle for the longest chains).

IV. RESULTS AND DISCUSSION

We consider first noninteracting solvents (i.e., nonbonded interactions between solvent beads are assumed zero, but double occupancy of sites is forbidden). The characteristics of the systems studied are summarized in Table I. The systems of group A are homogeneous chains X_n of variable length n at different densities. In the systems of group B the solvent molecule is $CXCC$. The molecules of group C are of the form $C(XCC)_n$, with variable length and densities as indicated in Table I. Molecules of group D, $C(XCCC)_n$, have a lower relative content of attraction sites X. ρ_X is the density of these sites in the system and zq_X is the number of nonbonded nearest neighbor (per chain) to these sites. zq_C is the number of nearest neighbors, per chain, to the C-sites.

Results of simulations with homogeneous chain solvents (group A) are shown in Fig. 1. Here the solvation energy $\mathscr{E}_I/\epsilon_{IX}$, which in this case is equal to N_{IX}, is plotted against $\epsilon_{IX}/(kT)$ for systems A2 and A4 (Table I). Shown are the simulation results, as well as results of the QCA, Eq. (8), and of the mean-field approximation for the solvent (MFAS), Eq. (10). The error bars shown here and in Fig. 2 represent the standard deviation of the energy from its average along the trajectory. The QCA is seen to be in excellent agreement with the numerical results while the MFAS shows slight deviations. In the present model the only source of error in the MFAS is in using r instead of q for the effective molecular length. For the cubic lattice this leads to a maximum deviation of less than 20% between the QCA and the MFAS results.

The same excellent agreement between the QCA and the numerical simulation results was found at the other densities and chain lengths (systems A in Table I). The QCA represents solvation in this model very well, despite its inherent seemingly gross simplifications. In the QCA correlations between beads belonging to the same chain are disregarded and the information about the chain connectivity enters only via the parameter zq, the number of nonbonded nearest neighbors.

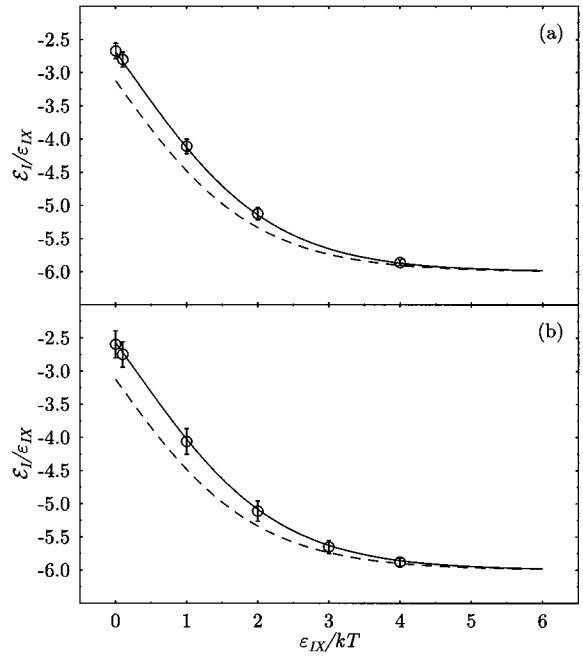

FIG. 1. Results from the MC simulations (circles), QCA (solid lines), and MFAS (dashed lines) for cases A2 (a) and A4 (b). Both systems are at a total density of $\rho=0.520$.

The agreement between the QCA equation, Eq. (8), and the numerical results is not as good for heterogeneous chains. Figures 2 display results for the solvation energy vs temperature for the systems B2, C2, and D2. These systems are characterized by the same total density, $\rho=0.52$ and different densities of the X (binding) sites. The deviations of the QCA from the ''exact'' numerical results are shown explicitly in Fig. 2(d), where the ratio $\mathcal{E}_I^{\rm sim}/\mathcal{E}_I^{\rm QCA}$ between the numerical and the QCA solvation energy is shown as a function of temperature. Similar results for the systems B3, C2, and D3 are shown in Fig. 3. These systems are characterized by approximately similar densities of X beads and different total densities.

Figures 4 and 5 compare the exact and the QCA results for solvents of the same kind. In Fig. 4 $\mathcal{E}_I^{\rm sim}/\mathcal{E}_I^{\rm QCA}$ is shown as a function of $\epsilon_{IX}/(kT)$ for the solvents B1, B2, and B3—$CXCC$ molecules at different densities. In Fig. 5 a similar plot is displayed for solvents B2, C1, C2, and C4—$C(XCC)_n$ at density $\rho\approx 0.52$. Figure 6 is similar to Fig. 5, using solvents of type $C(XCCC)_n$ (systems D1, D2, and D4).

Finally, from the dependence of the scaled solvation energy on the strength of the interaction ϵ_{IX}, and using Eq. (12), the free energy of solvation, A_I, and the corresponding entropy, S_I, can be calculated. Results are shown, for $\epsilon_{IX}/(kT)=6$ in Table II.

The following observations can be made on these results:

(1) The QCA provides a reasonable approximation to the thermodynamics of solvation in the present model, with the largest errors not exceeding ~20%.
(2) The QCA is virtually exact in the infinite temperature, $\epsilon_{IX}/(kT)\to 0$, limit. This is consistent with the success of the QCA for homogeneous solvent chains. In the zero temperature limit the QCA also produces for the present model the exact solvation energy, which corresponds to the configurations were all sites nearest to the solute are occupied by X beads.
(3) The QCA seems to work better at higher system densities and lower chain lengths. The effect of chain length seems to saturate beyond $n=2-3$ (see Figs. 5 and 6).

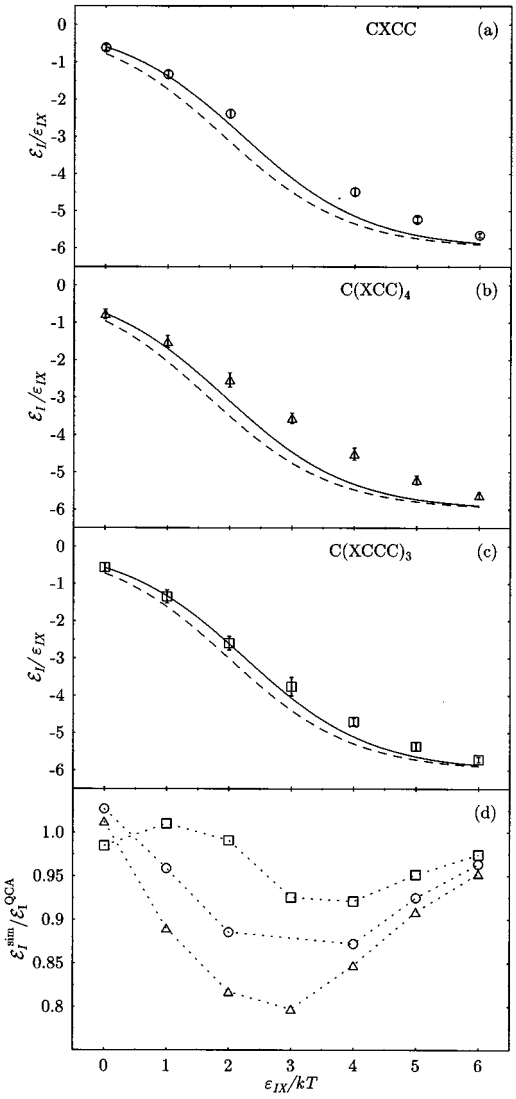

FIG. 2. Results from MC simulations for systems defined in Table I. B2 [○ in (a) and (d)], C2 [△ in (b) and (d)], and D2 [□ in (c) and (d)], together with the corresponding results using QCA (solid lines) and MFAS (dashed lines). These systems are characterized by the same value of $\rho=0.520$ and different values of ρ_X. (d) shows the ratio between the energies obtained from the simulations and from the QCA (○ for B2, △ for C2, and □ for D2). The dotted lines connecting the points in (d) and in Figs. 3–6 serve just to guide the eyes.

Figures 2–4 also provide a qualitative understanding of the inadequacies of the QCA. In the present model the solvation energy is determined by the number of pairs consisting of the ion and a binding site. The QCA provides a good approximation for this number in the case of homogeneous chains. For heterogeneous chains this approximation does

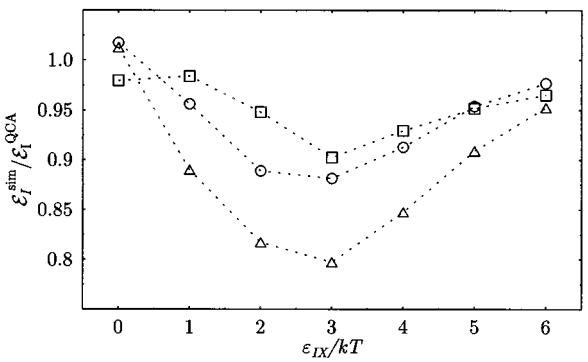

FIG. 3. Ratio between the energies obtained from the MC simulations and from the QCA for systems B3, C2, and D3 in Table I. (○, system B3; △, system C2; and □, system D3). All the systems have the approximately same density of X sites $\rho_X \approx 0.16$.

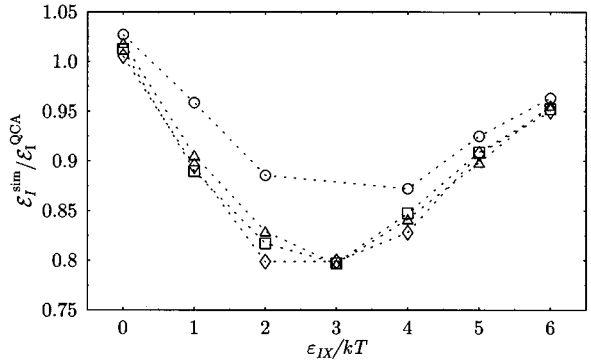

FIG. 5. Ratio between the energies obtained from the MC simulations and from the QCA for the solvents $C(XCC)_n$; $n=1,2,4,8$; at density $\rho \approx 0.52$ (○, system B2; △, system C1; □, system C2; and ◇, system C4).

not account well for the correlation between an $I-X$ pair and a third X bead. Such correlations arise from both intramolecular and intermolecular origins. Intermolecular correlations can be best understood by considering the case of chains with only one X bead per chain. The attachment of an X-bead to the impurity implies a larger concentration of C beads (originating from the same chain) near the impurity, therefore a smaller probability (smaller than if the chains were dismembered) for another X-bead to attach. Another statement of the same argument is that if two chains attach simultaneously to the ion the number of available configurations for each chain is reduced relative to the number of configurations available to a singly attached chain, thus creating an entropic effect which decreases the average N_{IX}. The exact solvation energy will therefore be smaller (in absolute value) than predicted by the QCA, as indeed seen in Figs. 2–4. The behavior of systems B (Fig. 4) is characteristic of such interchain correlation.

Intramolecular correlations arise from the specific geometry of the solvent molecules involved and the specific steric nature of the impurity-solvent bond (here determined by the lattice geometry). In the present model, linear chain molecules on a cubic lattice where the impurity as well as each bead occupies one lattice site, such correlations arise from the fact that in $C(XCC)_n$ chains two consecutive X beads cannot both attach to the impurity because of the geometrical restrictions. The solvation energy in $C(XCC)_n$ solvents is therefore expected to be even lower than expected on the basis of interchain correlations only. The opposite situation holds for $C(XCCC)_n$ chains. Here the attachment of one X-bead to the ion correlates positively (on our cubic lattice) with the attachment of the nearest neighbor X-bead on the same chain with the same ion (see Fig. 7). Therefore the solvation energy in this case will be higher than expected based on the interchain correlation alone. This difference between $C(XCC)_n$ and $C(XCCC)_n$ can be seen comparing Figs. 5 and 6.

Next consider the energy, free energy, and entropy of solvation. Table II shows the energy, $\mathscr{E}_I$, free energy, A_I, and the entropy, S_I, of solvation for the systems displayed in Table I, for the temperature $kT/\epsilon_{IX}=1/6$. The free energy was computed from Eq. (12) and $S_I=(\mathscr{E}_I-A_I)/T$. Note that at this temperature the sites neighboring to the ion are almost fully occupied by solvent X beads so $\mathscr{E}_I$ is close to its maximum value of 6. The entropy of solvation shows a strong dependence on the solvent density and a relatively week dependence on the solvent molecular size (for a given density). The biggest effect seen in Table II is the very different entropies of solvation between solvents with a different fraction

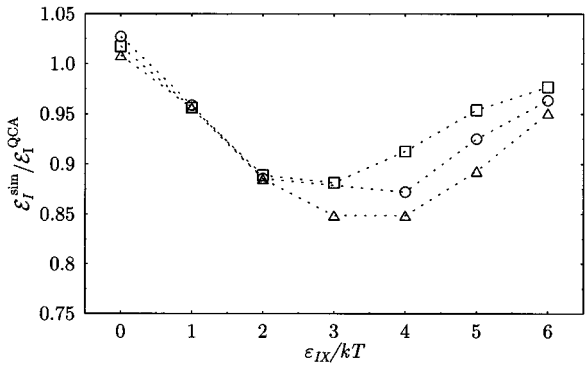

FIG. 4. Ratio between the energies obtained from the MC simulations and from the QCA for the systems B in Table I ($CXCC$ at different densities) (△, system B1; ○, system B2; and □, system B3).

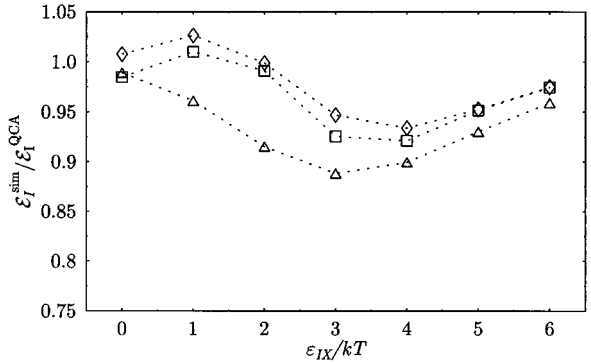

FIG. 6. Ratio between the energies obtained from the MC simulations and from the QCA for the solvents $C(XCCC)_n$; $n=2,3,6$; at density $\rho \approx 0.52$ (△, system D1; □, system D2; and ◇, system D4).

TABLE II. Thermodynamic quantities for solvation for $kT/\epsilon_{IX}=1/6$. The superscript (1) means that the thermodynamic values were obtained from the integration of the QCA results, Eqs. (8) or (9), using Eq. (12).

Label	ρ	ρ_X	$\mathscr{E}_I/\epsilon_{IX}$	A_I/ϵ_{IX}	S_I/k
A1$^{(1)}$	0.400	0.400	−5.97	−4.91	−6.39
A2$^{(1)}$	0.520	0.520	−5.98	−5.20	−4.69
A3$^{(1)}$	0.648	0.648	−5.99	−5.46	−3.19
A4$^{(1)}$	0.520	0.520	−5.98	−5.16	−4.95
A5$^{(1)}$	0.702	0.702	−5.99	−5.52	−2.80
B1	0.400	0.100	−5.53	−3.03	−15.0
B2	0.520	0.130	−5.65	−3.34	−13.9
B3	0.648	0.162	−5.76	−3.67	−12.5
C1	0.518	0.148	−5.63	−3.34	−13.7
C2	0.520	0.160	−5.62	−3.43	−13.2
C2$^{(1)}$	0.520	0.160	−5.90	−3.95	−11.7
C3	0.702	0.216	−5.79	−3.89	−11.4
C4	0.525	0.168	−5.61	−3.45	−13.0
D1	0.522	0.116	−5.61	−3.36	−13.7
D2	0.520	0.120	−5.71	−3.49	−13.3
D3	0.702	0.158	−5.70	−3.80	−11.4
D4	0.525	0.126	−5.72	−3.58	−12.9

of binding sites. Thus, for example, $S_I/k=-4.69$ for the solvent X_4 at density $\rho=0.52$ and $S_I/k=-13.9$ for the solvent $CXCC$ at the same overall density. Much of this effect is associated with the effective density of binding sites, as can be seen by considering a solvent of unconnected beads: For a solvent made of independent X and C beads at $\rho=0.52$ we calculate [using expressions provided in Ref. 2(a)] under the same condition $S_I/k=-3.83$ if all beads are X type and $S_I/k=-11.6$ if $\rho_X=0.130$ (as in solvent B2).

In addition to the noninteracting solvents considered so far, we have performed a limited set of simulations with the solvents characterized by attractive interactions between nonbonded nearest-neighbor beads. We note in passing that imposing strong attractive interactions between the chains may have a profound effect on the system structure as well as on its dynamical behavior. This is seen in Figs. 8 and 9 which for the solvent X_{13} display the vacancy pair correlation function $G(r)$ and the "time" (in terms of number of MC steps per particle) dependence of the mean square displacement of the chain's center of mass for three different values of the solvent bead–bead interaction ϵ_{bb};

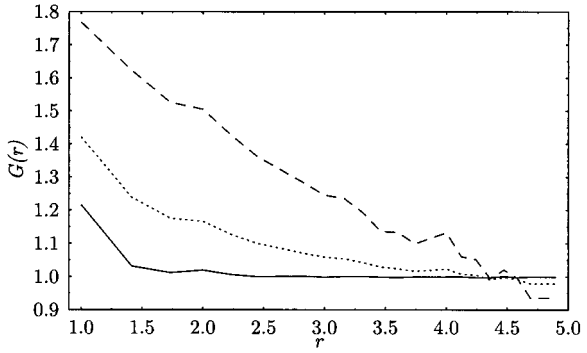

FIG. 8. Vacancy pair correlation function in the pure solvent X_{13} for different values of the bead–bead interaction, ϵ_{bb}. Solid line $\epsilon_{bb}/kT=0.1$, dotted line $\epsilon_{bb}/kT=0.5$, and dashed line $\epsilon_{bb}/kT=1.5$. The bead density is $\rho=0.52$.

$\epsilon_{bb}/kT=0.1$, 0.5, and 1.5. The drastic reduction in chain mobility for $\epsilon_{bb}/kT=1.5$ suggests that permanent immobile aggregates are formed in this system. Therefore the solvation studies described below were limited to systems with $\epsilon_{bb}/kT=0.1$ and $\epsilon_{bb}/kT=0.5$.

Note that for an interacting solvent the solute–solvent interaction energy $\mathscr{E}_I$, Eq. (8), does not represent the full solvation energy, ΔE_I, of species I since the solvent reorganization energy is not included. However, for the purpose of comparing to the QCA prediction we continue to consider this quantity.

For $\epsilon_{bb}/kT=0.1$, $\mathscr{E}_I$ is found to be virtually unchanged (within numerical errors) from the results obtained for $\epsilon_{bb}=0$; while for $\epsilon_{bb}/kT=0.5$ $\mathscr{E}_I$ differs by up to 15% from the noninteracting case. An interesting trend is seen in the performance of the QCA. Figures 10 and 11 show the ratio of the "exact" and the QCA results for $\mathscr{E}_I$ for two systems; X_{13} and $C(XCC)_4$ at $\rho=0.52$. For comparison the same results for systems A4 and C2 are shown. It is seen that while QCA is very accurate for noninteracting X_{13} solvent, its performance is somewhat reduced in the corresponding interacting $(\epsilon_{bb}/kT=0.5)$ solvent. In contrast, the relatively poor performance of the QCA in the noninteracting system is im-

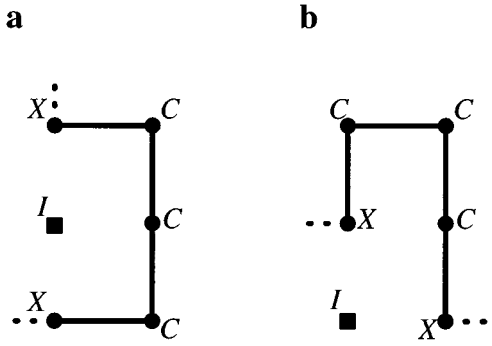

FIG. 7. Possible configurations of the $XCCCX$ segment about a central ion I showing the positive correlation in attaching two neighboring X-beads to the ion as discussed in the text.

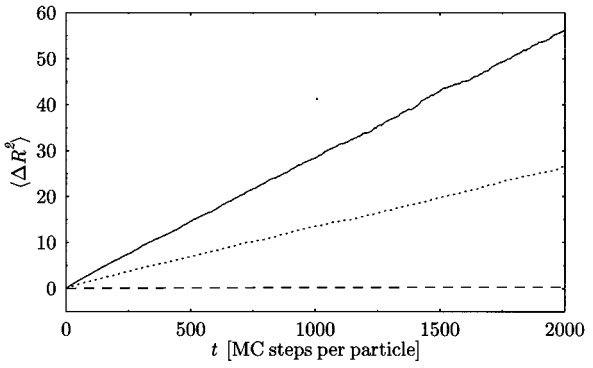

FIG. 9. Mean square displacement of the chain's (X_{13}) center of mass in terms of the number of MC steps per bead, for different values of ϵ_{bb}. Solid line $\epsilon_{bb}/kT=0.1$, dotted line $\epsilon_{bb}/kT=0.5$, and dashed line $\epsilon_{bb}/kT=1.5$. Bead density is $\rho=0.52$.

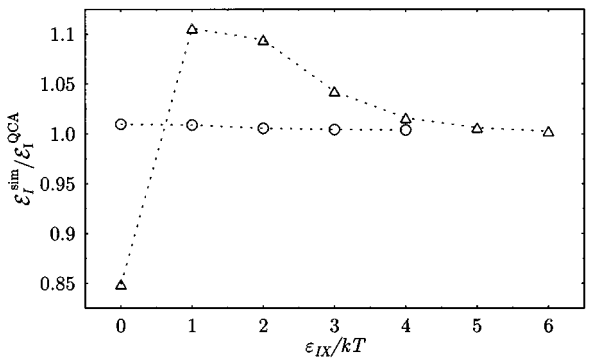

FIG. 10. Ratio between the energies obtained from the MC simulations and from the QCA for the solvent X_{13}, at density $\rho=0.52$, for interacting and noninteracting systems (○, $\epsilon_{bb}/kT=0.0$; △, $\epsilon_{bb}/kT=0.5$). The dotted lines connecting the points in Figs. 10 and 11 serve just to guide the eyes. Note that here (and in Fig. 11) the parameter ϵ_{IX}/kT is varied at constant temperature, and the intrachain interactions remain constant.

proved when interactions are present. The same trends were observed with shorter chain solvents.

These observations can be rationalized by noticing again that the QCA disregards three-body and higher correlations. Consider first the homogeneous X_{13} solvent (Fig. 10). When $\epsilon_{IX}<0.5kT=\epsilon_{bb}$ the solvent prefers the neighborhood of other solvent molecules, effectively ''rejecting'' the solute thus leading to a three-body contribution to the solvation energy which makes it smaller (in absolute value) than the QCA value which does not account for such correlations. For stronger ion–solvent interaction the ion attracts the solvent, and solvent–solvent attractions will further increase the solvent occupation of sites nearest-neighbor to the ion, beyond the QCA prediction. The QCA then somewhat underestimates the actual solvation energy as seen in Fig. 10.

For heterogeneous $C(XCC)_4$ solvent we have argued above that the effect of many-body correlations is to make the actual interaction energy lower (in absolute value) than the QCA prediction. The correlations imposed by the bead–bead attraction however work in the opposite direction since the attachment of one bead to the ion enhances the solvent density about the ion, hence the solvation energy. The relative success of the QCA in this case thus results from cancellation of opposing effects of many-body correlations.

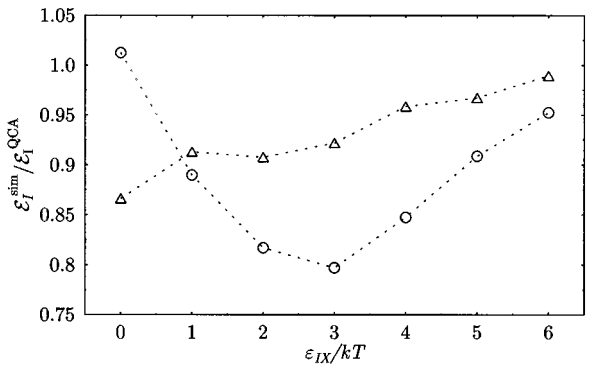

FIG. 11. Ratio between the energies obtained from the MC simulations and from the QCA for the solvent $C(XCC)_4$, at density $\rho=0.52$, for interacting and noninteracting systems (○, $\epsilon_{bb}/kT=0.0$; △, $\epsilon_{bb}/kT=0.5$).

V. CONCLUSIONS

The application of the (two-body) quasichemical approximation in the calculation of solvation energies in lattice models of solvation provides a reasonable approximation (error smaller than 20%) for all systems studied. Deviations from the QCA may be qualitatively explained in terms of many-body correlations.

APPENDIX: DERIVATION OF THE SOLVATION ENERGY

In this section we summarize the calculations for the standard (infinite dilution) free energy of solvation in the constant volume ensemble. The calculation is very similar to the one developed in Ref. 2(b) for the constant pressure ensemble, so we keep the description brief referring to Ref. 2(b) for the details.

The chemical potential of molecules of kind $i(\neq 0)$ in this ensemble is obtained from the derivative of the Helmholtz free energy A with respect to the amount of component i. This can be formally written in the form

$$\begin{aligned}\mu_i&=\left(\frac{\partial A}{\partial N_i}\right)_{T,V,\{N_j\}_{\neq 0,i}}\\&=\left[\left(\frac{\partial A}{\partial N_i}\right)_{T,V,\{N_j\}_{\neq i},\{N_{ij}\}}+\sum_i\sum_{j>i}\left(\frac{\partial A}{\partial N_{ij}}\right)_{T,V,\{N_j\},\{N_{lm}\}_{\neq ij}}\right.\\&\quad\cdot\left(\frac{\partial N_{ij}}{\partial N_i}\right)_{T,V,\{N_j\}_{\neq i},\{N_{lm}\}_{\neq ij}}+\left(\frac{\partial A}{\partial N_0}\right)_{T,V,\{N_j\}_{\neq 0},\{N_{ij}\}}\\&\quad\left.\cdot\left(\frac{\partial N_0}{\partial N_i}\right)_{T,V,\{N_j\}_{\neq 0,i},\{N_{ij}\}}\right].\end{aligned}\tag{A1}$$

From the QCA the second term on the right-hand side of Eq. (A1) is zero at equilibrium. Using Guggenheim's expression[3] for the entropy $S(\{N_i\},\{N_{ij}\})$ [e.g., Eq. (1) of Ref. 2(b)] and the energy $E(\{N_i\},\{N_{ij}\})=-\Sigma_{i=1}^{n}\Sigma_{j\geqslant i}^{n}N_{ij}\epsilon_{ij}$, and keeping in mind $M=\Sigma_{i=0}^{n}r_iN_i=V/v^*$, we get

$$\begin{aligned}\mu_i=&-\frac{z}{2}\,q_i\epsilon_{ii}+kT\left\{\ln N_i-\ln\frac{\delta_i}{\sigma_i}+\frac{z}{2}\,q_i\,\ln\left[\frac{2N_{ii}}{z(q_iN_i)^2}\right]\right\}\\&-r_ikT\left\{\ln N_0+\frac{z}{2}\ln\left[\frac{2N_{00}}{z(N_0)^2}\right]\right\},\end{aligned}\tag{A2}$$

where the parameters δ_i and σ_i are related to the number of configurations of a chain of kind i in the lattice. Equation (A2) can be rewritten in term of the scaled variables defined by Eq. (5) as

$$\mu_i = -\frac{z}{2} q_i \epsilon_{ii} + kT\left[\ln \frac{N_i}{M} - \ln \frac{\delta_i}{\sigma_i} - r_i \ln \frac{N_0}{M} + \frac{z}{2} (q_i - r_i) \ln \frac{M}{N_q} + \frac{z}{2} q_i \ln \frac{\chi_{ii}}{\varphi_i^2} - \frac{z}{2} r_i \ln \frac{\chi_{00}}{\varphi_0^2} \right]. \quad \text{(A3)}$$

This result can be shown to have the same form as the one obtained in Ref. 2(b) for μ_i using the isothermal–isobaric ensemble.[11] As in Ref. 2(b), we identify the infinite dilution limit of μ_I (i.e., $\lim_{\varphi_I \to 0} \mu_I$) as the standard free energy of solvation of species I, ΔA_I, in the solvent mixture. Disregarding the second and third terms in Eq. (A3),[2(b)] we are left with

$$\Delta A_I = -\frac{z}{2} q_i \epsilon_{II} + kT\left[+ \frac{z}{2} (q_I - r_I) \ln \frac{M^0}{N_q^0} - r_I \ln \frac{N_0^0}{M^0} + \frac{z}{2} q_I \lim_{\varphi_I \to 0} \ln \frac{\chi_{II}}{\varphi_I^2} - \frac{z}{2} r_I \ln \frac{\chi_{00}^0}{(\varphi_0^0)^2} \right], \quad \text{(A4)}$$

where the superscript 0 indicates quantities calculated for the pure solvent, i.e., with $\varphi_I = 0$ (while subscript 0 indicates properties evaluated for the "vacancy species"). Using Eq. (18) of Ref. 2(b),

$$\lim_{\varphi_I \to 0} \ln \frac{\chi_{II}}{\varphi_I^2} = -2 \ln\left(\sum_i{}' \; e^{-1/2 \Delta \epsilon_{Ii}/kT} \sqrt{\chi_{ii}^0} \right), \quad \text{(A5)}$$

where Σ_i' denotes summation over all $i \neq I$ (including $i = 0$), and repeating manipulations of the kind used in Ref. 2(b), we finally get

$$\Delta A_I = kT\left[\frac{z}{2} (q_I - r_I) \ln \frac{M^0}{N_q^0} - r_I \ln \frac{N_0^0}{M^0} + \frac{z}{2} (q_I - r_I) \ln \frac{\chi_{00}^0}{(\varphi_0^0)^2} - z q_I \ln\left(\sum_i{}' \; e^{\epsilon_{Ii}/kT} \frac{\chi_{0i}^0}{\varphi_0^0} \right) \right]$$
$$= \Delta A_I' - kT z q_I \ln\left(\sum_i{}' \; e^{\epsilon_{Ii}/kT} \frac{\chi_{0i}^0}{\varphi_0^0} \right), \quad \text{(A6)}$$

where $\Delta A_I'$, the term which survives if $\epsilon_{Ii} = 0$ for all i, is the cavity formation term.[2(b)] The corresponding solvation energy is obtained from

$$\Delta E_I = \left(\frac{\partial \beta \Delta A_I}{\partial \beta} \right)_{V,\{N_m\}} = \left(\frac{\partial \beta \Delta A_I}{\partial \beta} \right)_{V,\{N_m\},\{N_{ij}\}} + \sum_i{}' \sum_{j>i}{}' \left(\frac{\partial \beta \Delta A_I}{\partial N_{ij}} \right)_{T,V,\{N_m\},\{N_{lm}\} \neq ij} \cdot \left(\frac{\partial N_{ij}}{\partial \beta} \right)_{V,\{N_m\},\{N_{lm}\} \neq ij}. \quad \text{(A7)}$$

The first term of the right-hand side of Eq. (A7) leads after some algebra to Eq. (9). For the free energy derivative appearing on the second term of Eq. (A7) we find, using Eq. (A6), that $[\partial(\beta \Delta A_I)/\partial N_{ij}] = 0$ if $i,j \neq 0$, while

$$\left(\frac{\partial \beta \Delta A_I}{\partial N_{0j}} \right)_{T,V,\{N_m\},\{N_{lm}\} \neq 0j} = -\frac{z}{2} (q_I - r_I) \cdot \frac{1}{N_{00}} - z q_I \frac{e^{\epsilon_{Ij}/kT}}{\Sigma_m{}' \chi_{0m}^0 e^{\epsilon_{Im}/kT}}. \quad \text{(A8)}$$

Also, using Eq. (1) we get

$$\left(\frac{\partial N_{0j}}{\partial \beta} \right)_{V,\{N_m\},\{N_{lm}\} \neq 0j} = -\epsilon_{jj} \left(\frac{2}{N_{0j}} + \frac{1}{N_{jj}} + \frac{1}{N_{00}} \right)^{-1}. \quad \text{(A9)}$$

For noninteracting chains $\epsilon_{jj} = 0$ for all j, therefore the second term of Eq. (A7) vanishes, leading to Eq. (9). Finally note that the cavity formation term, $\Delta A_I'$ in Eq. (A6) is not calculated in the MC computation and therefore should be omitted when comparing the QCA and the simulation results.

ACKNOWLEDGMENTS

This research was supported in part by the Kurt Lion Foundation. The research of A.N. is also supported by the Israel National Science Foundation.

[1] For solvation and association of ions in polymer hosts, see, e.g., (a) F. M. Gray, *Solid Polymer Electrolytes* (VCH, New York, 1991); (b) L. M. Torell and S. Schantz, in *Polymer Electrolyte Reviews*, edited by J. MacCallum and C. A. Vincent (Elsevier, New York, 1988), Vol. II; (c) S. Schantz, L. M. Torell, and J. R. Stevens, J. Chem. Phys. **94**, 6862 (1991); (d) L. M. Torell, P. Jacobson, and G. Peterson, Polym. Adv. Technol. **4**, 152 (1993).

[2] (a) R. Olender and A. Nitzan, J. Chem. Phys. **100**, 705 (1994) (paper I of this series); (b) **101**, 2338 (1994) (paper II of this series).

[3] E. A. Guggenheim, Proc. R. Soc. London, Ser. A **183**, 213 (1944).

[4] E. A. Guggenheim, *Mixtures* (Oxford University, Oxford, 1952).

[5] J. A. Barker, J. Chem. Phys. **20**, 1526 (1952).

[6] W. H. Press, B. P. Flannery, S. A. Teukolsky, and W. T. Vetterling, *Numerical Recipies* (Cambridge University, Cambridge, 1989), Sec. (9.6).

[7] As is customary in lattice gas theories we use the term "noninteracting chains" for the situation where only site exclusion interactions exist between the chains.

[8] Note that the present case of constant volume is different from the constant pressure situation considered in Ref. 2, although the final expression, Eq. (10) can be shown to be the same in a system of noninteracting solvent molecules.

[9] A. Baumgärtner, in *Monte Carlo Method in Condensed Matter Physics*, edited by K. Binder (Springer, Berlin, 1993), Chap. 9.

[10] J. Skolnick and A. Kolinski, Adv. Chem. Phys. **78**, 223 (1990).

[11] In Ref. 2, substituting the expression for the pressure [Eq. (13)] in Eq. (16) for μ_i, the form of Eq. (A3) above is obtained.